

**UNCLASSIFIED**

**AD 433172**

**DEFENSE DOCUMENTATION CENTER**

**FOR**

**SCIENTIFIC AND TECHNICAL INFORMATION**

**CAMERON STATION, ALEXANDRIA, VIRGINIA**



**UNCLASSIFIED**

NOTICE: When government or other drawings, specifications or other data are used for any purpose other than in connection with a definitely related government procurement operation, the U. S. Government thereby incurs no responsibility, nor any obligation whatsoever; and the fact that the Government may have formulated, furnished, or in any way supplied the said drawings, specifications, or other data is not to be regarded by implication or otherwise as in any manner licensing the holder or any other person or corporation, or conveying any rights or permission to manufacture, use or sell any patented invention that may in any way be related thereto.

64-10

433172 EDL-M623

DA 36-039 AMC-00088(E)  
NO. 30 OF 110 COPIES

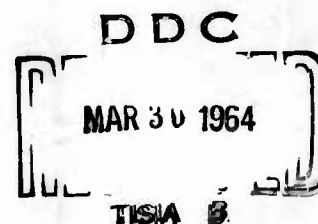
CATALOGED BY DDC

AS AD No. \_\_\_\_\_

433172

# Log Periodic Dipole Array with Parasitic Elements

NORMAND BARBANO



SYLVANIA ELECTRONIC SYSTEMS  
Government Systems Management  
for GENERAL TELEPHONE & ELECTRONICS



## ELECTRONIC DEFENSE LABORATORIES

MOUNTAIN VIEW, CALIFORNIA

PREPARED FOR THE UNITED STATES ARMY

DEFENSE DOCUMENTATION CENTER  
AVAILABILITY NOTICE

QUALIFIED REQUESTORS MAY OBTAIN  
COPIES OF THIS REPORT FROM THE  
DEFENSE DOCUMENTATION CENTER

**U S ARMY ELECTRONICS RESEARCH UNIT  
POST OFFICE BOX 205  
MOUNTAIN VIEW, CALIFORNIA**

**DISTRIBUTION LIST FOR EDL PUBLICATION: M 623**

COMMANDING OFFICER US ARMY ELECTRONICS RESEARCH UNIT P O BOX 205 MOUNTAIN VIEW, CALIFORNIA	101	CHIEF OF STAFF US AIR FORCE ATTN: AFRSTB WASHINGTON, D. C. 20390	1301	DIRECTOR NATIONAL SECURITY AGENCY ATTN: C3/TDL FORT GEORGE G. MEADE, MARYLAND	2502
COMMANDING GENERAL US ARMY MATERIEL COMMAND ATTN: AMCRD-DE-E-E WASHINGTON 25, D. C.	201	DEPUTY C/S FOR MILITARY OPNS DEPARTMENT OF THE ARMY ATTN: ORGN R&D BRANCH WASHINGTON, D. C. 20390	1401	COMMANDER AF CAMBRIDGE RESEARCH LABORATORY ATTN: CRREL HANSCOM FIELD BEDFORD, MASSACHUSETTS	2601
TECHNICAL LIBRARY, OASD-R&D ROOM 3E1C65, THE PENTAGON WASHINGTON, D. C. 20390	301	DIRECTOR US NAVAL RESEARCH LABORATORY COUNTERMEASURES BRANCH CODE 5430 WASHINGTON 25, D. C.	1501	COMMANDING OFFICER US ARMY ELECTRONICS R&D LABORATORIES ATTN: SELRA/ADJ FORT MONMOUTH, NEW JERSEY	2701
COMMANDING OFFICER HARRY DIAMOND LABORATORIES ATTN: LIBRARY WASHINGTON 25, D. C.	401	CENTRAL INTELLIGENCE AGENCY ATTN: LIAISON DIV, OCD 2430 E STREET NW WASHINGTON 25, D. C.	1601	COMMANDING OFFICER US ARMY ELECTRONICS R&D LABORATORIES ATTN: SELRA/GFR FORT MONMOUTH, NEW JERSEY	2801
CHIEF OF NAVAL OPERATIONS DEPARTMENT OF THE NAVY ATTN: OP 347 WASHINGTON 25, D. C.	501	US ATOMIC ENERGY COMMISSION DIVISION OF MILITARY APPLICATION ATTN: CLASSIFIED TECH LIBRARY 1901 CONSTITUTION AVE., NW WASHINGTON 25, D. C.	1701	COMMANDING OFFICER US ARMY ELECTRONICS R&D LABORATORIES ATTN: SELRA/SE FORT MONMOUTH, NEW JERSEY	2901
CHIEF, BUREAU OF SHIPS DEPARTMENT OF THE NAVY ATTN: CODE 818 WASHINGTON 25, D. C.	601	CHIEF OF RESEARCH & DEVELOPMENT OCS, DEPARTMENT OF THE ARMY WASHINGTON 25, D. C.	1801	MARINE CORPS LIAISON OFFICER ATTN: SELRA/LNR U S ARMY ELECTRONICS R&D LABORATORIES FORT MONMOUTH, NEW JERSEY	3001
CHIEF BUREAU OF WEAPONS, RAAV DEPARTMENT OF THE NAVY WASHINGTON, D. C. 20390	701	CHIEF, US ARMY SECURITY AGENCY ARLINGTON HALL STATION ARLINGTON 12, VIRGINIA	1901	COMMANDING OFFICER US ARMY ELECTRONICS MATERIEL SUPPORT AGENCY, ATTN: SELMS/ES-ADJ FORT MONMOUTH, NEW JERSEY	3101
CHIEF BUREAU OF NAVAL WEAPONS DEPARTMENT OF THE NAVY ATTN: CODE R-12 WASHINGTON, D. C. 20390	801	DEPUTY PRESIDENT US ARMY SECURITY AGENCY BOARD ARLINGTON HALL STATION ARLINGTON 12, VIRGINIA	2001	COMMANDING GENERAL US ARMY ELECTRONICS COMMAND ATTN: AMSEL-EW FORT MONMOUTH, NEW JERSEY	3201
OFFICE OF NAVAL RESEARCH DEPARTMENT OF THE NAVY ATTN: CODE 427 WASHINGTON, D. C. 20390	901	DEFENSE DOCUMENTATION CENTER FOR SCIENTIFIC & TECHNICAL INFO-DDC CAMERON STATION ALEXANDRIA, VIRGINIA	21020	COMMANDER ROME AIR DEVELOPMENT CENTER ATTN: RAALD GRIFFITHS AFB ROME, NEW YORK	3401
DIRECTOR US NAVAL RESEARCH LABORATORY ATTN: CODE 2027 WASHINGTON, D. C. 20390	1001	CHIEF US ARMY SECURITY AGENCY ATTN: IALOG-ESE ARLINGTON HALL STATION ARLINGTON 12, VIRGINIA	2201	REDSTONE SCIENTIFIC INFO CENTER US ARMY MISSILE COMMAND REDSTONE ARSENAL, ALABAMA	3505
CENTRAL INTELLIGENCE AGENCY ATTN: OCR MAIL ROOM WASHINGTON, D. C. 20505	1102	COMMANDING OFFICER USA FOREIGN SCIENCE & TECHNOLOGY CENTER ATTN: AMXST-PP-CB MUNITIONS BUILDING WASHINGTON, D. C. 20315	2301	AIR FORCE MISSILE TEST CENTER AFMTC-MTBAT PATRICK AFB, FLORIDA	36001
CHIEF OF STAFF US AIR FORCE ATTN: DCS/D AFOP-00 WASHINGTON 25, D. C.	1201	COMMANDER TACTICAL AIR COMMAND REGION LANGLEY AFB, VIRGINIA	2401	AIR FORCE MISSILE TEST CENTER AFMTC TECH LIBRARY-MU 135 PATRICK AFB, FLORIDA	37001

18 MARCH 1964

CONTINUED ON REVERSE SIDE

<p>COMMANDER AIR PROVING GROUND COMMAND ATTN: APGC-PGAPI EGLIN AFB, FLORIDA</p>	3801	<p>COMMANDING GENERAL US ARMY ELECTRONICS PROVING GROUND ATTN: AG TECHNICAL LIBRARY FORT HUACHUCA, ARIZONA</p>	5101
<p>COMMANDER AERONAUTICAL SYSTEMS DIVISION AIR FORCE SYSTEMS COMMAND ATTN: ASRNCC-1 WRIGHT-PATTERSON AFB, OHIO</p>	3901	<p>COMMANDER PACIFIC MISSILE RANGE ATTN: LIBRARIAN POINT MUGU, CALIFORNIA</p>	5201
<p>COMMANDER WRIGHT AIR DEVELOPMENT DIVISION ATTN: WWRNRE-4 WRIGHT-PATTERSON AFB, OHIO</p>	4001	<p>COMMANDER NAVAL ORDNANCE TEST STATION ATTN: TEST DIRECTOR - CODE 30 INYO KERN, CHINA LAKE, CALIFORNIA</p>	5301
<p>COMMANDER WRIGHT AIR DEVELOPMENT DIVISION AERONAUTICAL SYSTEMS DIVISION ATTN: ASRNRE-4 WRIGHT-PATTERSON AFB, OHIO</p>	4101	<p>COMMANDING OFFICER &amp; DIRECTOR US NAVY ELECTRONICS LABORATORY SAN DIEGO 52, CALIFORNIA</p>	5401
<p>COMMANDER WRIGHT AIR DEVELOPMENT DIVISION ATTN: ASRNCF1 WRIGHT-PATTERSON AFB, OHIO</p>	4202	<p>STANFORD ELECTRONICS LABORATORY STANFORD UNIVERSITY ATTN: W. R. RAMBO STANFORD, CALIFORNIA</p>	5501
<p>PRESIDENT US ARMY AIR DEFENSE BOARD ATTN: IDRS FORT BLISS, TEXAS</p>	4401	<p>SCIENTIFIC &amp; TECHNICAL INFO FACILITY ATTN: NASA REP (SAK/DL-925) P O BOX 5700 BETHESDA, MARYLAND 20014</p>	5601
<p>DIRECTOR COMMUNICATIONS &amp; ELECTRONICS AIR DEFENSE COMMAND ENT AIR FORCE BASE COLORADO SPRINGS, COLORADO</p>	4501	<p>COMMANDING OFFICER US ARMY COMBAT DEVELOPMENTS COMMAND COMMUNICATIONS - ELECTRONICS AGENCY ATTN: CAGCE-ESE FORT HUACHUCA, ARIZONA</p>	5701
<p>COMMANDER AF MISSILE DEVELOPMENT CENTER ATTN: MISSILE COUNTERMEASURES LABORATORY HDLV HOLLOMAN AFB, NEW MEXICO</p>	4601	<p>DIRECTOR USA ENGINEER GEODESY INTELLIGENCE AND MAPPING R&amp;D AGENCY ATTN: ENGGM-SS FORT BELVOIR, VIRGINIA</p>	5801
<p>COMMANDING OFFICER US ARMY ELECTRONICS R&amp;D ACTIVITY ATTN: SELWS/W WHITE SANDS MISSILE RANGE, N.M.</p>	4701		
<p>COMMANDER, FIELD COMMAND DEFENSE ATOMIC SUPPORT AGENCY AIR DEVELOPMENT DIVISION SANDIA BASE ALBUQUERQUE, NEW MEXICO</p>	4801		
<p>COMMANDING OFFICER US ARMY ELECTRONICS R&amp;D ACTIVITY ATTN: SELHU-EE FORT HUACHUCA, ARIZONA</p>	5001		

EDL-M623

ELECTRONIC DEFENSE LABORATORIES

P. O. BOX 205  
Mountain View, California

TECHNICAL MEMORANDUM

No. EDL-M623  
30 January 1964

LOG PERIODIC DIPOLE ARRAY WITH PARASITIC ELEMENTS

Normand Barbano

Approved for Publication . . . . B. Lamberty  
Manager  
Antenna Department

K. Walton  
Head  
Antenna Systems Section

Prepared for the U. S. Army Electronics Research and  
Development Laboratory under Contract DA 36-039 AMC-00088 (E).

SYLVANIA ELECTRIC PRODUCTS, INC.

CONTENTS

<u>Section</u>	<u>Title</u>	<u>Page</u>
1.	ABSTRACT . . . . .	1
2.	INTRODUCTION . . . . .	1
3.	GENERAL DISCUSSION . . . . .	2
4.	UNIFORM DIPOLE ARRAY WITH PARASITIC ELEMENTS . . . . .	8
5.	LOG PERIODIC DIPOLE ARRAY WITH PARASITIC ELEMENTS . . . . .	13
5.1	Single Parasitic Element Design . . . . .	13
5.2	Multiparasitic Element Design . . . . .	15
6.	LOG PERIODIC MONOPOLE ARRAY WITH PARASITIC ELEMENTS . . . . .	22
6.1	UHF Model . . . . .	22
6.2	Microwave Model . . . . .	29
7.	CONCLUSION . . . . .	35
8.	REFERENCES . . . . .	36



ILLUSTRATIONS

<u>Figure</u>	<u>Title</u>	<u>Page</u>
1.	Two Methods of Feeding an Array of Log Periodic Dipoles . . . . .	3
2.	k- $\beta$ Diagram for the Two Methods of Feeding an Array of Log Periodic Dipoles . . . . .	5
3.	Parameters Used to Define a Log Periodic Dipole Array. . . . .	6
4.	Uniform Dipole Array with Parasitic Elements . . . . .	9
5.	Model of a Uniform Dipole Array with Parasitic Elements ( $s/l = 0.2$ ) . . . . .	10
6.	Brillouin Diagram for Uniform Dipole Array with Parasitic Elements ( $s/l = 0.2$ ) . . . . .	11
7.	Parameters Used to Define a Log Periodic Dipole Array with Parasitic Elements . . . . .	14
8.	Log Periodic Dipole Array with Parasitic Elements - - Single Parasitic Element Design ( $\tau = 898$ , $s/l = 0.113$ ) . . . . .	16
9.	Impedance of a Log Periodic Dipole Array with Parasitic Elements ( $\tau = 0.898$ , $s/l = 0.113$ ) . . . . .	17
10.	Dipole Array with Parasitic Elements ( $\tau = 0.898$ , $s/l = 0.113$ ) . . . . .	18
11.	Log Periodic Dipole Array with Parasitic Elements - - Dual Parasitic Element Design . . . . .	20
12.	E-plane Radiation Power Patterns of Log Periodic . . . . .	21
13.	Comparison of Log Periodic Dipole and Monopole Arrays with Parasitic Elements . . . . .	23
14.	Log Periodic Monopole Array with Parasitic Elements. . . . .	24

ILLUSTRATIONS -- Continued

<u>Figure</u>	<u>Title</u>	<u>Page</u>
15.	VSWR vs. Frequency for a Log Periodic Monopole with Parasitic Elements ( $\tau = 0.886$ , $s/\ell = 0.0568$ ) . . . . .	26
16.	E-plane Radiation Power Patterns of a Log Periodic Monopole Array with Parasitic Elements ( $\tau = 0.886$ , $s/\ell = 0.0568$ ) . . . . .	27
17.	H-plane Radiation Power Patterns of a Log Periodic Monopole Array with Parasitic Elements (20-degree conical cut) ( $\tau = 0.889$ , $s/\ell = 0.0568$ ) . . . . .	28
18.	Microwave Model of a Log Periodic Monopole Array with Parasitic Elements ( $\tau = 0.898$ , $s/\ell = 0.0557$ ) . . . . .	30
19.	E-plane Radiation Power Patterns of a Log Periodic Monopole Array with Parasitic Elements ( $\tau = 0.898$ , $s/\ell = 0.0557$ ) . . . . .	32
20.	H-plane Radiation Power Patterns of a Log Periodic Monopole Array with Parasitic Elements ( $\tau = 0.898$ , $s/\ell = 0.0557$ ) . . . . .	33

## LOG PERIODIC DIPOLE ARRAY WITH PARASITIC ELEMENTS

Normand Barbano

### 1. ABSTRACT.

The design and measured characteristics of dipole and monopole versions of a log periodic array with parasitic elements are discussed. In a dipole array with parasitic elements, these elements are used in place of every alternate dipole, thereby eliminating the need of a twisted feed arrangement for the elements to obtain log periodic performance of the antenna. This design with parasitic elements lends itself to a monopole version of the antenna which has a simplified feeding configuration. The result is a log periodic antenna design that can be used from high frequencies through microwave frequencies.

### 2. INTRODUCTION.

This report concerns modifying the design of a log periodic dipole antenna fed in phase progression such that the antenna will produce backfire radiation and operate in a pseudofrequency independent manner. The modification consists basically of replacing every alternate dipole element with a parasitic element of the same length. The resulting configuration is a log periodic dipole array which incorporates driven and parasitic elements with the same design ratio,  $\tau$ , and element-spacing-to-element-length ratio,  $s/l$ , as the initial antenna.

The characteristics of the modified antenna are discussed below, along with results of measurements taken on antenna models using one or two parasitic elements per cell. It is shown that the dipole array images exactly over a perfect ground plane to form a log periodic monopole array with parasitic elements. Special tuning networks or transmission-line coupling networks are shown to be unnecessary with this monopole array. Using measured data, the antenna's performance is discussed.

### 3. GENERAL DISCUSSION.

Co-planar log periodic dipole arrays have been in existence since 1960, when D. E. Isbell published an article illustrating a method of feeding the elements of the array in a phase reversal rather than a phase progression manner.<sup>1</sup> This phase reversal method of feeding the structure resulted in a log periodic array with pseudofrequency independent characteristics. The radiation patterns are unidirectional and linearly polarized in the direction of the dipoles. The beamwidths are constant over the entire bandwidth of the antenna. The input impedance is nearly constant with frequency.

Figure 1 illustrates the two methods of feeding the log periodic dipole array: phase progression and phase reversal. In the first method, the elements on one side of the structure are attached to one side of the two-wire transmission-line feeder, and the other elements are attached to the second wire of the transmission-line feeder. Since these elements are closely spaced, the phase of the current in adjacent elements will progress along the structure with respect to the feed, as shown in Figure 1A. A lagging phase condition is set up along the structure, with the result that a forward wave is excited and end-fire radiation occurs.

When the method of feeding the structure by phase reversal is employed, the result is backfire radiation. From Figure 1B, it can be seen that by alternately connecting each adjacent element to the opposite side of the transmission-line feeder, a phase reversal of  $\pi$  radians is introduced between each element. A backward wave can now be supported, since a leading phase condition exists along the structure with respect to the feed. This backward wave causes the backward radiation from the antenna.

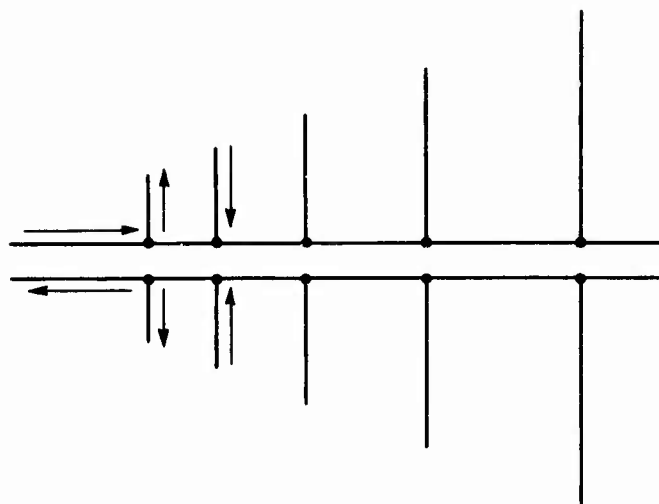
Since the conception of the log periodic dipole antenna, the use of the Brillouin diagram for analyzing periodic structures has been extended to log periodic antennas.<sup>2,3,4</sup> The Brillouin diagram shows the relationship of the phase constant on a periodic structure,  $\beta$ , to the intrinsic phase constant of free space,  $k$ , such that

$$\beta = \frac{2\pi}{\lambda_g}, \quad (1)$$

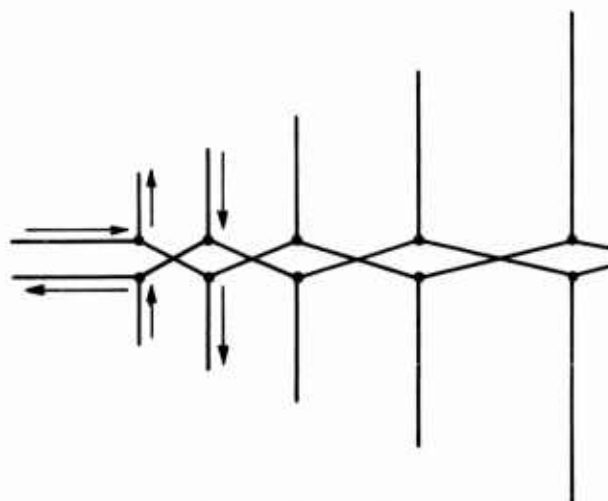
and

$$k = \frac{2\pi}{\lambda_0}, \quad (2)$$

1. See list of References in Section 8.



A. PHASE PROGRESSION METHOD



B. PHASE REVERSAL METHOD

Figure 1. Two Methods of Feeding an Array of Log Periodic Dipoles.

### 3. -- Continued.

where  $\lambda_g$  = wavelength of the bound wave on the uniform structure, and

$\lambda_0$  = free-space wavelength.

The  $k$ - $\beta$  version of the Brillouin diagrams for the two methods of feeding an array of log periodic dipoles is shown in Figures 2A and 2B.<sup>5, 6</sup> These plots are normalized with respect to the distance,  $d$ , along a unit cell of a uniform structure. The  $k$ - $\beta$  diagram for the uniform structure using the phase progression method of feeding the dipoles is shown in Figure 2A. The dashed curve shows the variation of  $kd$  versus  $\beta d$ . Note that  $\beta$  is always positive. This indicates that a lagging phase condition prevails on the structure relative to the feed point for all frequencies. Therefore, the wave on the structure propagates in the forward direction, and only end-fire radiation can be expected to occur. In contrast, the diagram for the uniform dipole structure fed with the phase reversal method shows a region where  $\beta$  is negative (Figure 2B). In this region of the diagram, the phase along the structure relative to the feed is leading. A backward wave will be supported and backfire radiation will occur. The region between the 45-degree slopes ( $kd = \pm \beta d$ ) drawn in the figures indicates where the wave on the structure is loosely bound. It is within this region that radiation is most likely to occur on a log periodic structure. These diagrams serve to verify the earlier conclusions made about the two methods of feeding the log periodic dipole arrays.

### DESIGN PARAMETERS.

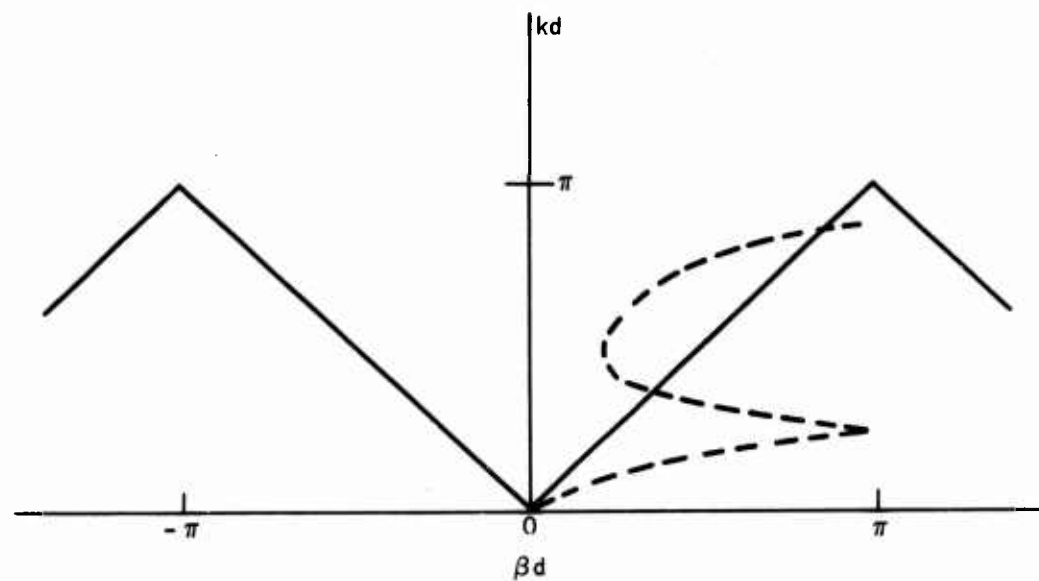
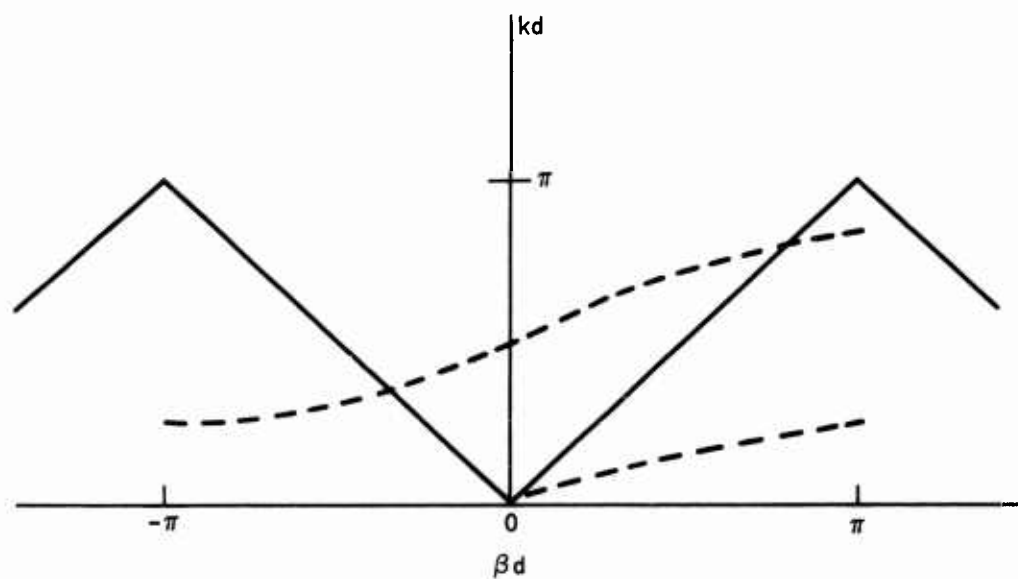
For reference, the parameters used in the design of a log periodic dipole antenna are now discussed. The structure is completely defined by the geometric ratio,  $\tau$ , and the element-spacing-to-element-length ratio,  $s/\ell$ . As apparent in Figure 3, the geometric ratio gives the growth rate of the elements and spacings by the following relationships:

$$\tau = \frac{\ell_n}{\ell_{n+2}} = \frac{x_n}{x_{n+2}}, \quad (3)$$

or

$$\sqrt{\tau} = \frac{\ell_n}{\ell_{n+1}} = \frac{x_n}{x_{n+1}}, \quad (4)$$

where  $x_n$  is the distance from the apex of the antenna to the  $n$ th element.

A.  $k$ - $\beta$  DIAGRAM FOR ANTENNA USING PHASE PROGRESSION METHODB.  $k$ - $\beta$  DIAGRAM FOR ANTENNA USING PHASE REVERSAL METHODFigure 2.  $k$ - $\beta$  Diagram for the Two Methods of Feeding an Array of Log Periodic Dipoles.

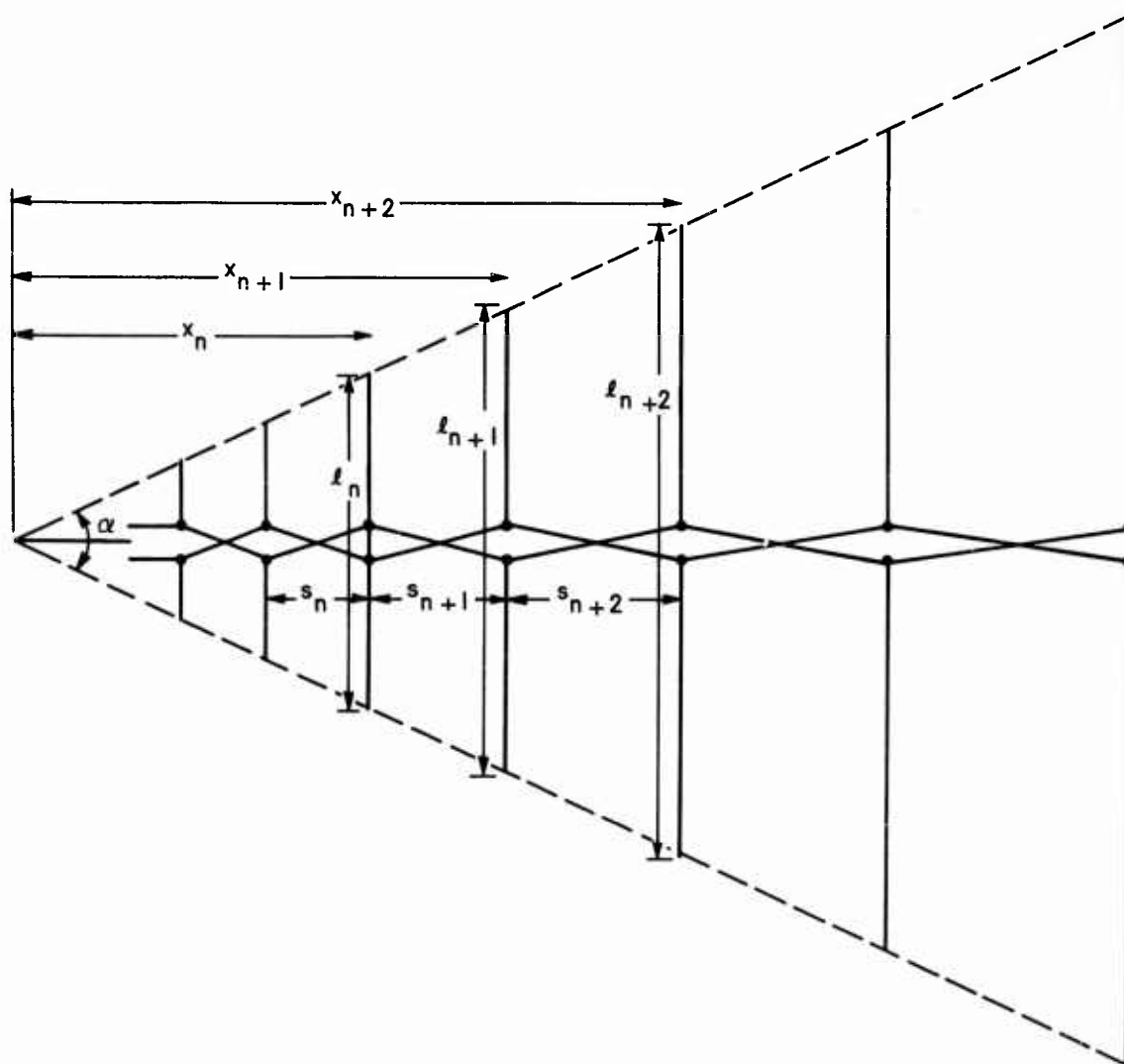


Figure 3. Parameters Used to Define a Log Periodic Dipole Array.



3. -- Continued.

The element-spacing-to-element-length ratio is given by

$$\frac{s_n}{\ell_n} = \frac{(1 - \sqrt{\tau})}{2 \tan \frac{\alpha}{2}}, \quad (5)$$

where  $\alpha$  is the included angle at the apex of the structure. Therefore,

$$\alpha = 2 \tan^{-1} \frac{\ell_n}{2 x_n}. \quad (6)$$

The largest and smallest values of  $\ell_n$  limit the bandwidth of the antenna -- the lowest frequency by the longest element and the highest frequency by the shortest element. The structure can be truncated at both ends without causing any serious degradation of antenna performance. Different values of  $\tau$  will change the radiation pattern characteristics somewhat.<sup>7</sup> A high value will give a narrower E-plane and H-plane radiation pattern beamwidth, a higher gain, and a larger front-to-back ratio. The impedance increases with a smaller value of  $\tau$  and angle  $\alpha$ .

#### 4. UNIFORM DIPOLE ARRAY WITH PARASITIC ELEMENTS.

As a preliminary examination of the log periodic dipole array with parasitic elements, consider a uniform array of driven and parasitic elements, as illustrated in Figure 4. Its construction consists of a two-wire transmission-line feeder with the dipole elements connected in a fashion similar to that shown in Figure 1A (the phase progression method of feeding a log periodic dipole array). The input to the feeder is electrically balanced. Parasitic elements are placed between the dipole elements to obtain a current phase reversal of  $\pi$  radians from one element to the next. This phase reversal is a primary requirement for obtaining a pseudo frequency-independent operation of the antenna.

A uniform dipole array with parasitic elements 24 inches long was constructed to determine its Brillouin ( $k-\beta$ ) diagram and radiation patterns associated with the diagram. This structure, shown in Figure 5, has resonant elements near 490 Mc. An element spacing of 2.4 inches ( $0.1\lambda$  at 490 Mc) was used. This array was designed to have a 50-ohm input impedance at the design frequency. The characteristic impedance of this uniform array was found to be dependent primarily upon the transmission-line feeder characteristics and also upon the element-spacing-to-element-length ratio,  $s/l$ .

Near-field phase measurements for the  $k-\beta$  diagram were taken along the feeder transmission line of the structure over the frequency range of 50 to 1000 Mc, and radiation patterns were measured over the corresponding frequency range. From these measurements, the phase constant,  $\beta$ , is determined. If a unit cell on the structure is defined to be the region from one driven element to the next along the feeder line, then the Brillouin diagram can be normalized in terms of a unit cell distance,  $d$ . The diagram for the uniform structure is shown in Figure 6 as having the normalized coordinates,  $kd$  and  $\beta d$ . This diagram contains a few of the measured E-plane radiation patterns at discrete frequencies.

The Brillouin curve begins at the origin at zero frequency and extends through the forward wave region,  $0 \leq \beta d \leq \pi$ , with increasing frequency. In this region, the phase along the feeder line lags the reference phase at the input terminals, and end-fire radiation occurs as shown by the radiation patterns. As the curve approaches the boundary,  $\beta d = \pi$ , radiation in both the end-fire and backward directions occurs, indicating that both the forward and backward waves are excited on the structure. The curve now extends into the backward-wave region,  $\pi \leq \beta d \leq 2\pi$ , where a leading phase distribution exists on the feeder line. Backward-wave radiation now occurs as shown in Figure 6. In the region where  $kd \geq -(\beta d - 2\pi)$ , the surface wave on the structure is loosely bound; however, the wave is tightly bound in the region where  $kd \leq -(\beta d - 2\pi)$ . The curve then proceeds to cross the

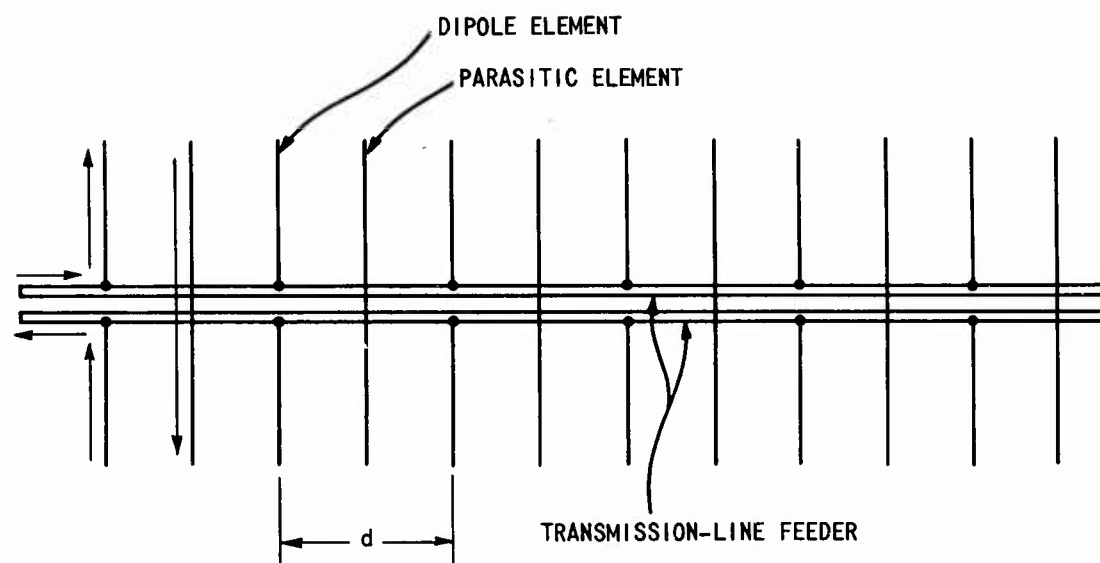


Figure 4. Uniform Dipole Array with Parasitic Elements.



63091801

Figure 5. Model of a Uniform Dipole Array with Parasitic Elements ( $s/l=0.2$ ).

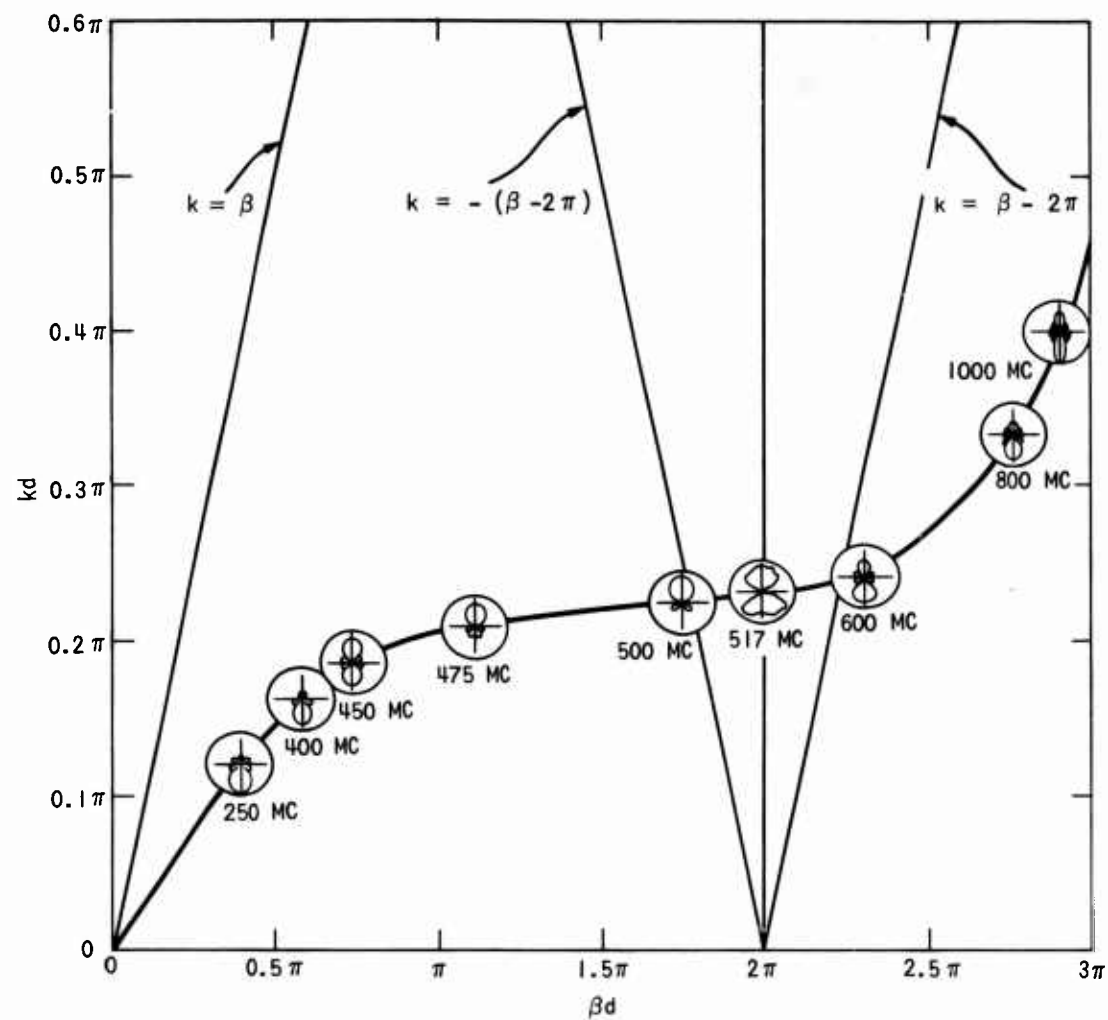


Figure 6. Brillouin Diagram for Uniform Dipole Array with Parasitic Elements ( $s/l = 0.2$ ).

## 4. -- Continued.

boundary,  $\beta d = 2\pi$ , into the forward-wave region,  $2\pi \leq \beta d \leq 3\pi$ . The wave is still loosely bound in this region. At the intersection with the line,  $\beta d = 2\pi$ , radiation in both the end-fire and backward directions occurs once again on the structure, as shown in Figure 6. The region,  $2\pi \leq \beta d \leq 3\pi$ , is then entered, and end-fire radiation occurs once again with the wave tightly bound.

The Brillouin diagram shows that a log periodic dipole array with parasitic elements is capable of stable, pseudo frequency-independent operation. A Brillouin diagram for a particular uniform array can be used to predict the performance of other similar arrays, provided the element-length-to-element spacing,  $s/l$ , is kept constant. This constancy is achieved by scaling the coordinates,  $kd$  and  $\beta d$ , to compensate for the difference in the element lengths.

The active region of a log periodic antenna occurs where the electrical length of the elements is nearly a half-wavelength; thus it can be seen that the  $k-\beta$  diagram of a uniform array with elements of equivalent length predicts that backfire-radiation will most likely occur at this frequency. For example, if a log periodic array having an  $s/l$  ratio of 0.2 is fed with a 490-Mc signal, then the diagram of Figure 6 will apply. It is apparent that the points on the curve corresponding to this frequency lie in the backward-radiation region of the diagram. A close investigation of the frequency bandwidth in the radiation region of Figure 6 shows that it is narrower than that of a conventional log periodic dipole antenna. This indicates that the equivalent circuit for the active region of the dipole array with parasitic elements has a higher effective  $Q$ . From this information, it can be predicted that a higher density of elements (a larger value of  $\tau$ ) is required for the log periodic dipole array with parasitic element design than for the conventional dipole array design. As will be seen below, this requirement becomes necessary for successful operation of the antenna.

## 5. LOG PERIODIC DIPOLE ARRAY WITH PARASITIC ELEMENTS.

### 5.1 Single Parasitic Element Design.

A log periodic dipole array with a single parasitic element will be considered in this section. The antenna is a co-planar type antenna designed such that each alternate element can be considered to be a driven element, with parasitic elements located in between these driven elements. The design parameters for this structure,  $\tau$  and  $s/\ell$ , are identical to a conventional log periodic dipole array. The variables used with these parameters are defined in Figure 7. The antenna utilizes a two-wire transmission-line feeder with a balanced input, with the input being located at the end having the shortest elements. The driven elements are connected to the feeder line, and the parasitic elements are unattached, as described in the discussion on the uniform array. The length and spacing between each adjacent element is a function of the geometric ratio,  $\tau$ , and the element-spacing-to-element-length ration,  $s/\ell$ , as given by Equations (3) and (5), respectively.

The parasitic elements essentially are located at the position normally occupied by the active elements that connect to the opposite sides of the transmission line in a conventional log periodic dipole array. The parasitic elements produce the same effect as the driven dipole elements that they replace; that is, they introduce a constant phase shift of  $\pi$  radians between elements. A parasitic element, when located in the active region of the antenna, receives its energy primarily by the mutual coupling between it and the active elements. To some extent, mutual-coupling effects also exist between parasitic elements. Energy is not coupled to the parasitic elements capacitively from the feeder line. To verify this, experiments were performed in which the spacing between the parasitic elements and the transmission-line feeder was varied. No evidence of capacitive coupling was noted, since the experimental results showed negligible changes in the antenna characteristics.

Several models of the dipole array with parasitic elements were constructed for evaluation. These antennas were found to have a pseudofrequency independent operation. Their radiation patterns have constant beamwidths, and their input impedance is nearly constant over the entire frequency range of the antennas. It was noted that on models having too low a value of  $\tau$  and angle  $\alpha$ , the antenna ceased to function in a pseudo frequency-independent manner. With large element spacings, the mutual coupling between the parasitic elements and the active elements is reduced to a value below which the reradiated energy from the parasitic element is insufficient to act as an equivalent source. When the antenna operates properly, it behaves as if its apparent phase center moves along the structure with frequency such that, over a period, the phase

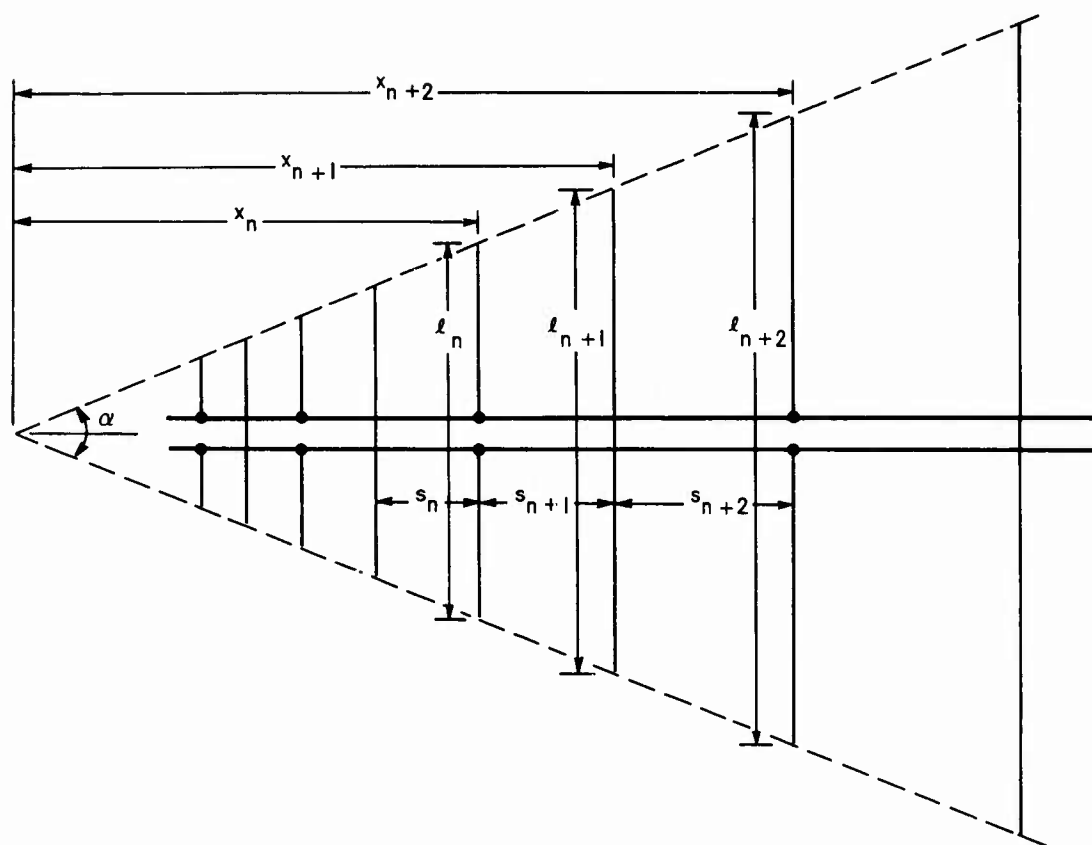


Figure 7. Parameters Used to Define a Log Periodic Dipole Array with Parasitic Elements.



### 5.1 -- Continued.

center will change continuously and smoothly from the driven element to the parasitic element, and finally to the next driven element.

A model of the dipole array with parasitic elements which has the design parameters,  $\tau = 0.898$  and  $s/\ell = 0.113$ , is shown in Figure 8. The shortest element of the structure (an active element) is 5.60 inches long, and the longest element (a parasitic element) is 12.54 inches long. The antenna is fed with an infinite balun constructed in one of the transmission-line feeders. A coaxial line with a characteristic impedance of 50 ohms was used.

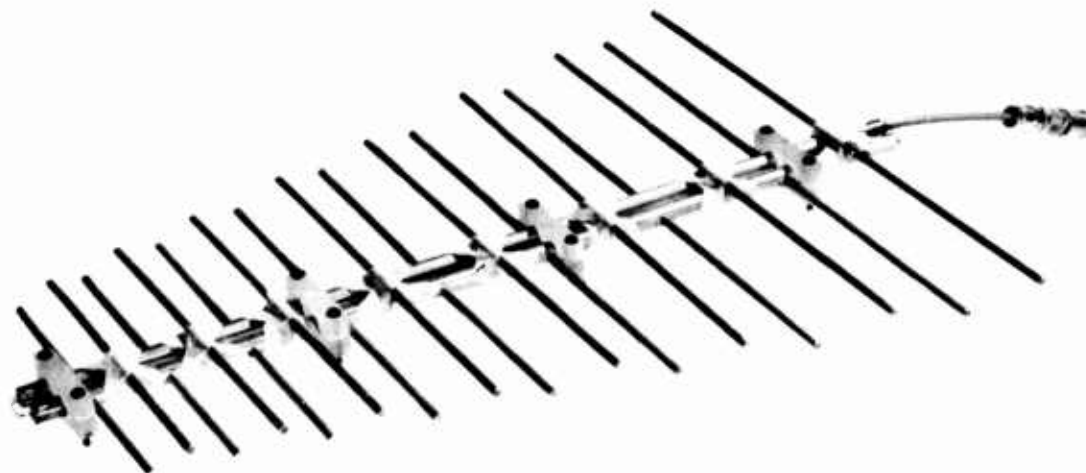
The impedance characteristics of this antenna over a full period are shown in Figure 9. The impedance circles approximately 25 ohms with a VSWR of 2:1 over the frequency range of 600 to 700 Mc. The low value of impedance occurs because of the number proximity of the parasitic element to the driven element. This effect is similar to that experienced with a dipole antenna having a driven and a reflecting parasitic element.

The radiation power patterns in the plane of the electric field are shown in Figure 10. These patterns have essentially a constant beamwidth of 60 degrees and a front-to-back ratio of 15 db or better. The radiation patterns are well-behaved over the frequency bandwidth of the antenna, as evident in Figure 10, and no radiation pattern degradation is experienced because of the parasitic elements in this antenna design.

### 5.2 Multiparasitic Element Design.

The next logical development of the log periodic dipole antenna with parasitic elements is a model having more than one parasitic element in a cell (a cell being defined in this case as the distance from one driven element to the next adjacent driven element). To investigate this interesting possibility, a dipole array with only a single parasitic element, and having the design parameters,  $\tau = 0.9$  and  $s/\ell = 0.201$ , was constructed. This antenna was tested and found to work satisfactorily in accordance with the behavior described in Section 5.1.

The next experiment involved modifying this antenna by adding to it a second complete set of parasitic elements. These elements were cut to the same length as the existing parasitic elements and placed on the antenna such that there were two parasitic elements of the same length between the driven elements or cells. The relative spacing of these elements in each cell was varied by the same percentage to obtain the best impedance and radiation characteristics of the antenna. The best design resulted in a spacing for the



63060739

Figure 8. Log Periodic Dipole Array with Parasitic Elements --  
Single Parasitic Element Design ( $\tau = 898$ ,  $s/\ell = 0.113$ ).

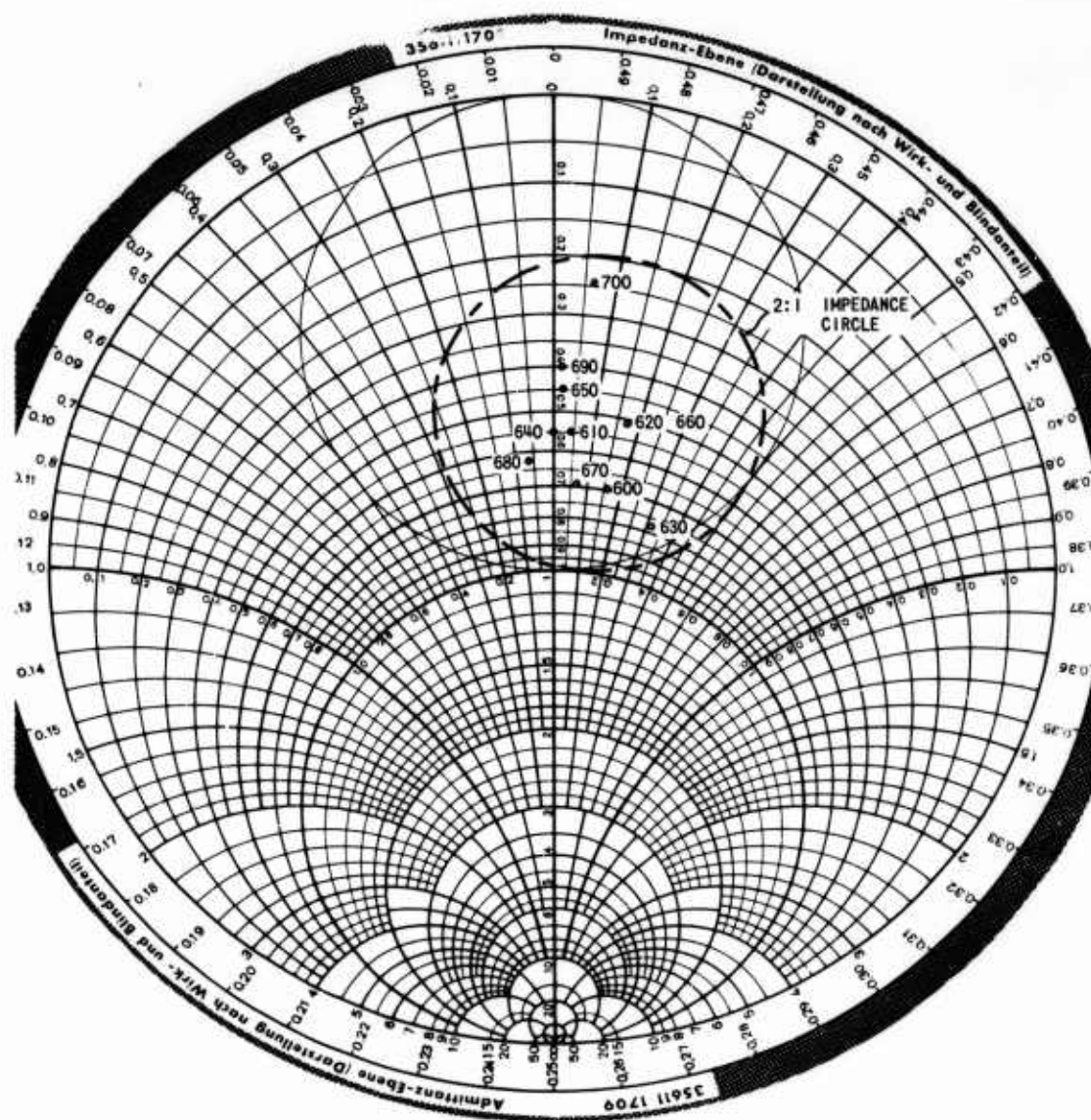


Figure 9. Impedance of a Log Periodic Dipole Array with Parasitic Elements ( $\tau = 0.898$ ,  $s/l = 0.113$ ).

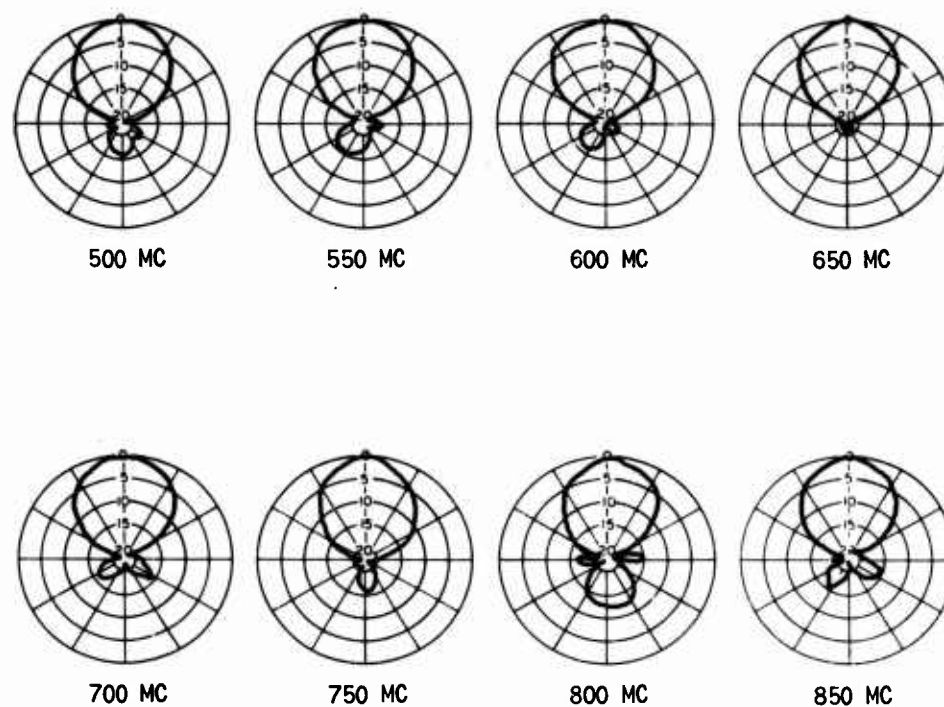
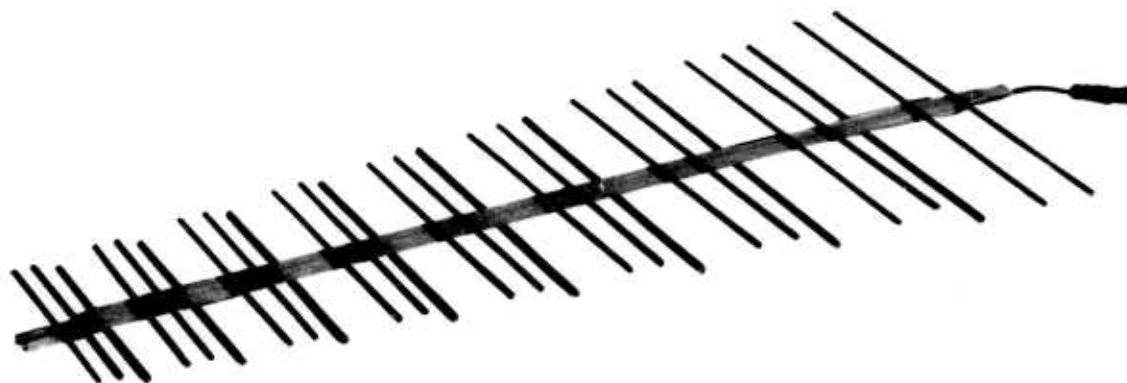


Figure 10. E-plane Radiation Power Patterns of a Log Periodic Dipole Array with Parasitic Elements ( $\tau = 0.898$ ,  $s/l = 0.113$ ).

5.2      -- Continued.

first parasitic element of 43 percent of the distance along a cell as measured from the shortest driven element in that cell, and a spacing for the second element of 68 percent of the distance along the same cell. The antenna of this design is shown in Figure 11. The original spacing between the driven elements is unchanged from the initial model and is spaced in accordance to the geometric ratio,  $\tau = 0.95$ . It can be seen from Figure 11 that the log periodic configuration is maintained from cell to cell and that the antenna is no longer periodic from element to element.

The measured radiation power patterns in the electric field plane of the antenna are shown in Figure 12. The radiation pattern shape is constant with frequency and has half-power beamwidths of 50 degrees in the E-plane and 60 degrees in the H-plane (not shown). Gain measurements greater than 10 db above isotropic were obtained on this model. One of the most significant improvements of this antenna as compared to the same antenna with only a single parasitic element per cell is an increase in the front-to-back ratio. An improvement of 5 db or greater is achieved, giving a front-to-back ratio equal to or greater than 20 db.



63070509

Figure 11. Log Periodic Dipole Array with Parasitic Elements -- Dual Parasitic Element Design.

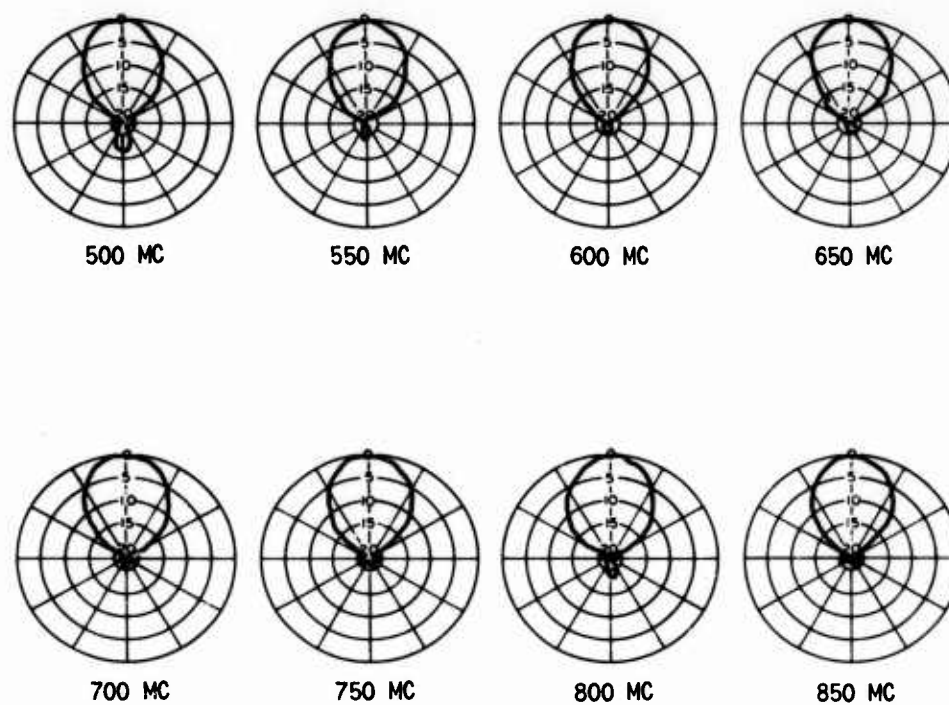


Figure 12. E-plane Radiation Power Patterns of Log Periodic.

## 6. LOG PERIODIC MONOPOLE ARRAY WITH PARASITIC ELEMENTS.

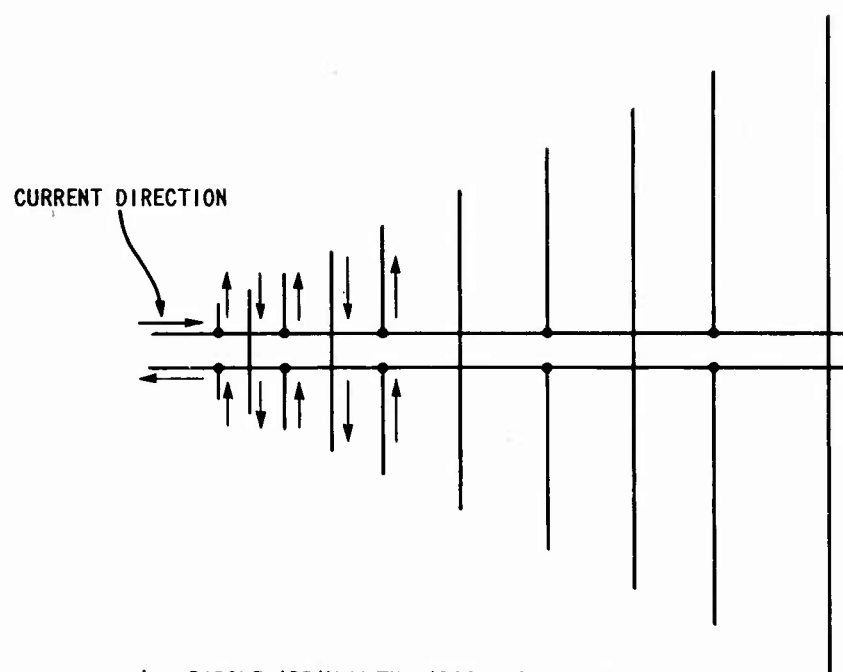
Because of the nature of the transmission-line feeder used with the conventional log periodic dipole array, the antenna cannot be imaged exactly over a ground plane to form a log periodic monopole array.<sup>9</sup> As a result, it became necessary to develop techniques for introducing the proper amount of phase shift between the monopole elements required for log periodic operation.<sup>10</sup> Successful operating models of log periodic monopoles are now in existence, but none of these antennas result in a configuration that conforms to a true image of the log periodic dipole array.

In this respect, the log periodic dipole array with parasitic elements lends itself to imaging with a ground plane to form a monopole array with parasitic elements. Figure 13A shows the current directions on the forward section of the log periodic dipole array with parasitic elements. The lower figure (Figure 13B) shows half of this antenna over a ground plane and its current distribution over the same region of the antenna as Figure 13A. The current along the transmission-line feeder of the monopole array has an image in the ground plane with the current direction reversed. The driven elements of the monopole are connected to the feeder line. For this arrangement, the image consists of monopole elements connected to the imaged feeder line. The current in these imaged elements is in the same direction as the actual elements themselves. The parasitic monopole elements are connected to the ground plane, and the image of these elements connects with the actual elements to form an equivalent continuous element with a unidirectional current distribution. Therefore, it can be seen from Figure 13 that the monopole antenna and its image, along with the removal of the ground plane, corresponds exactly to the dipole form of the antenna with parasitic elements.

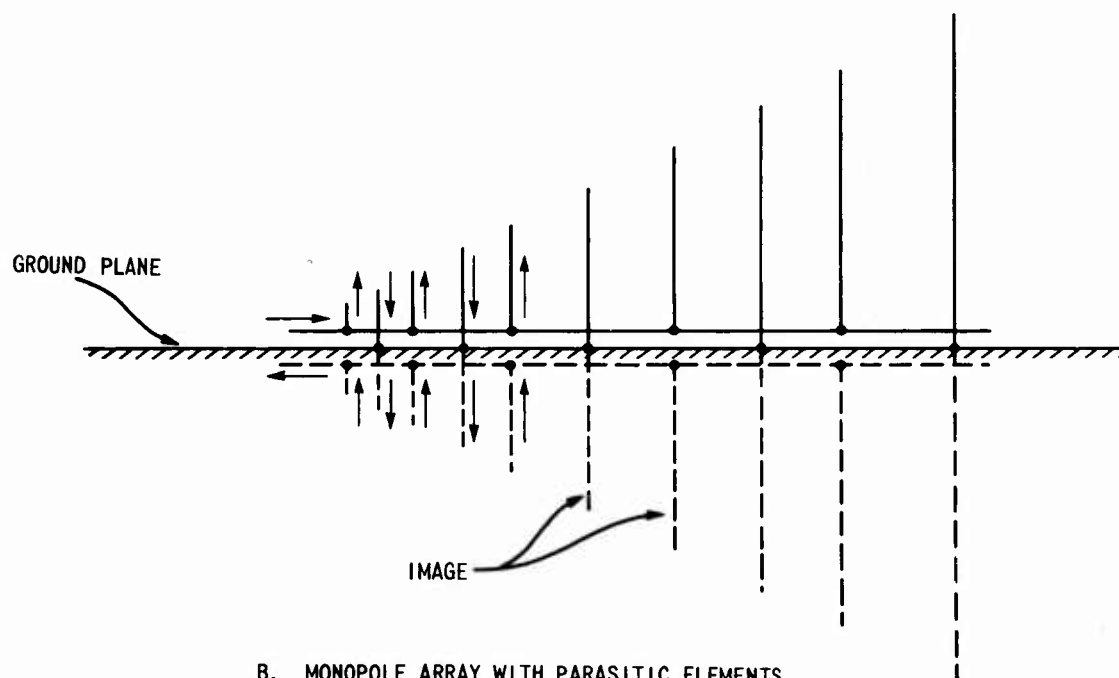
### 6.1 UHF Model.

A UHF model of the log periodic monopole array with parasitic elements (see Figure 14) was constructed for evaluation. This antenna consists of a metallic ground plane over which is placed a transmission feeder line. This line is fed with the inner conductor of a coaxial line as shown in Figure 14. The outer conductor of the coaxial line makes electrical contact with the surface of the ground plane. The driven elements are attached to the feeder line, and the parasitic elements are placed in between the driven elements and electrically connected to the ground plane. A design ratio,  $\tau$ , of 0.886 was used for this UHF model, and an element-spacing-to-element-length ratio,  $s/l$ , of 0.0568 was used.





A. DIPOLE ARRAY WITH PARASITIC ELEMENTS.



B. MONOPOLE ARRAY WITH PARASITIC ELEMENTS.

Figure 13. Comparison of Log Periodic Dipole and Monopole Arrays with Parasitic Elements.

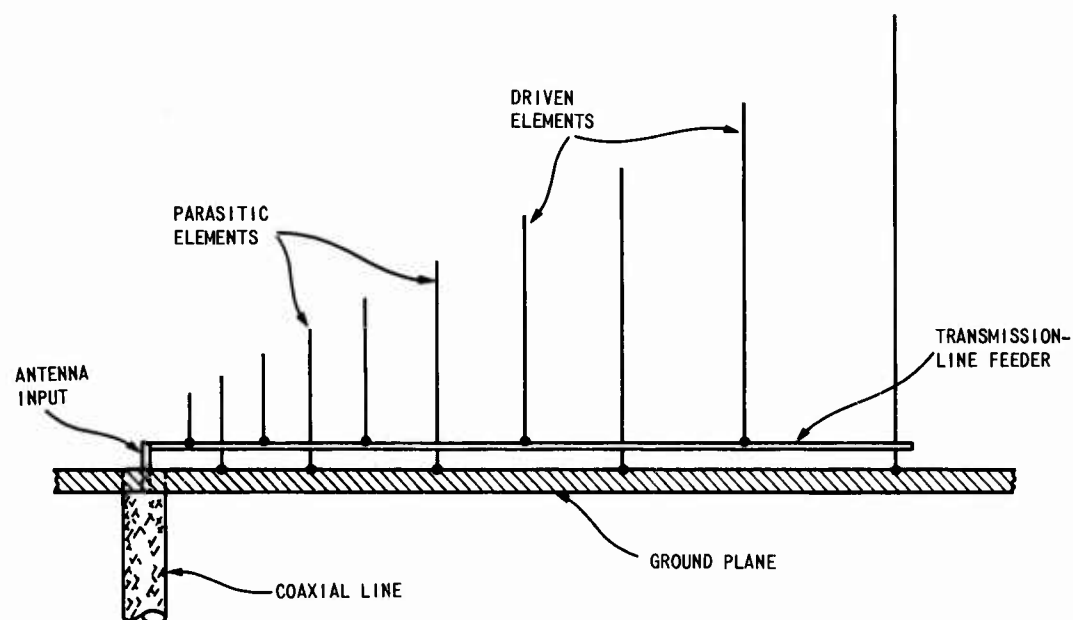


Figure 14. Log Periodic Monopole Array with Parasitic Elements.

### 6.1 -- Continued.

The VSWR of the antenna was measured with respect to 50 ohms for different transmission-line-to-ground-plane spacings. The following configurations were tried:

- (a) uniform transmission-line-to-ground-plane spacing (1/16 inch), and uniform transmission-line-to-parasitic-element spacing (1/16 inch);
- (b) uniform transmission-line-to-ground-plane spacing (1/16 inch), and tapered transmission-line-to-parasitic-element spacing (tapered from 1/16 inch at feed end to 3/16 inch at opposite end);
- (c) tapered transmission-line-to-ground-plane spacing (tapered from 1/16 inch at feed end to 3/16 inch at opposite end), and uniform transmission-line-to-parasitic-element spacing (1/16 inch).

The results of the VSWR measurements as a function of frequency for these various configurations are shown in Figure 15. A good match is shown to exist between the antenna and the coaxial line feed for all three configurations. It is important to note that the VSWR is nearly insensitive to the variations in the transmission-line-to-parasitic-element spacings. This behavior serves as evidence that the parasitic elements are excited by mutual coupling effects rather than by capacitive coupling.

This antenna operates in a pseudofrequency independent manner. A few of the measured E-plane and H-plane (20-degree conical cut) radiation power patterns of this antenna are shown in Figures 16 and 17. It can be seen that the radiation-pattern shapes remain essentially constant with frequency. The half-power beamwidths are 38 degrees in the E-plane and 120 degrees in the H-plane. These radiation patterns have a front-to-back ratio of 15 db.

In its simplicity of feeding, this antenna has the advantage over other log periodic monopole designs. No balun transformer is required, no critical spacing between the transmission-line feeder and the ground plane or parasitic elements exists, and no capacitive coupling to the elements is involved.

A second model of the monopole array with parasitic elements was constructed using a smaller value of  $\tau$  and a larger value of  $s/l$ . A value of  $\tau$  equal to 0.807 and  $s/l$  equal to 0.104 was used. This antenna did not operate in a frequency-independent manner. There was radiation pattern breakup at the frequencies where the main source of radiation appeared at the parasitic

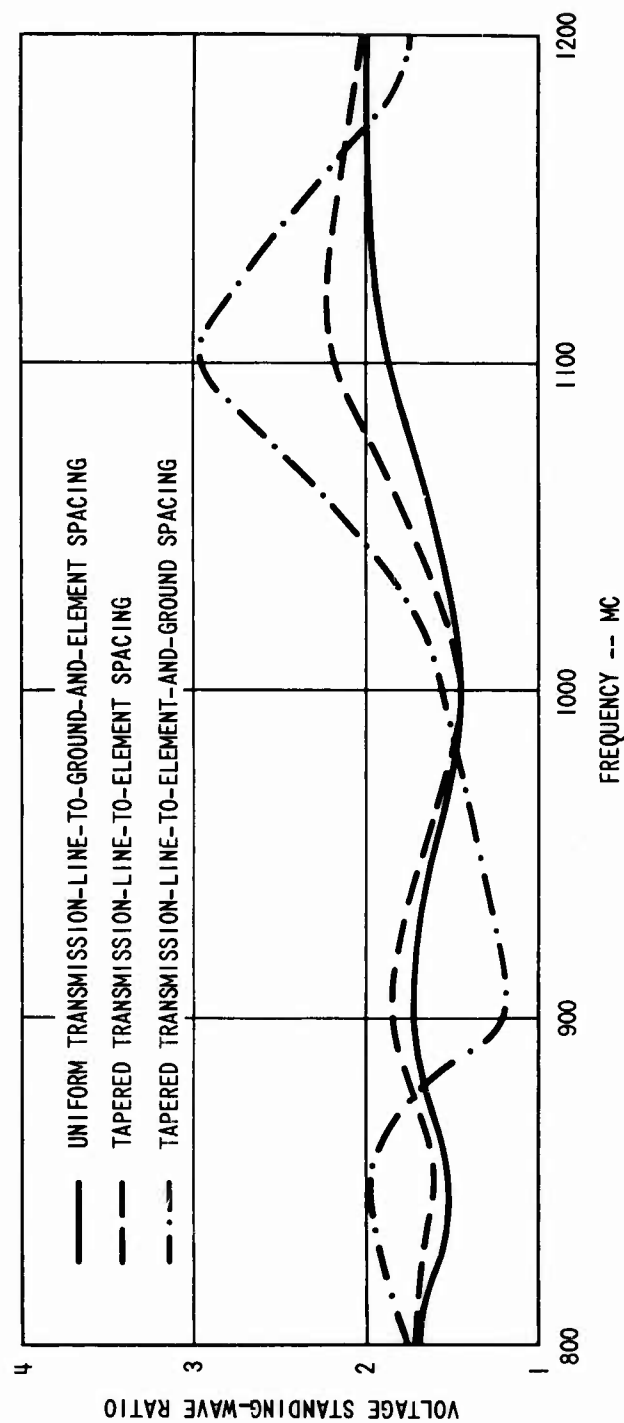


Figure 15. VSWR vs. Frequency for a Log Periodic Monopole with Parasitic Elements ( $\tau \approx 0.886$ ,  $s/l \approx 0.0568$ ).

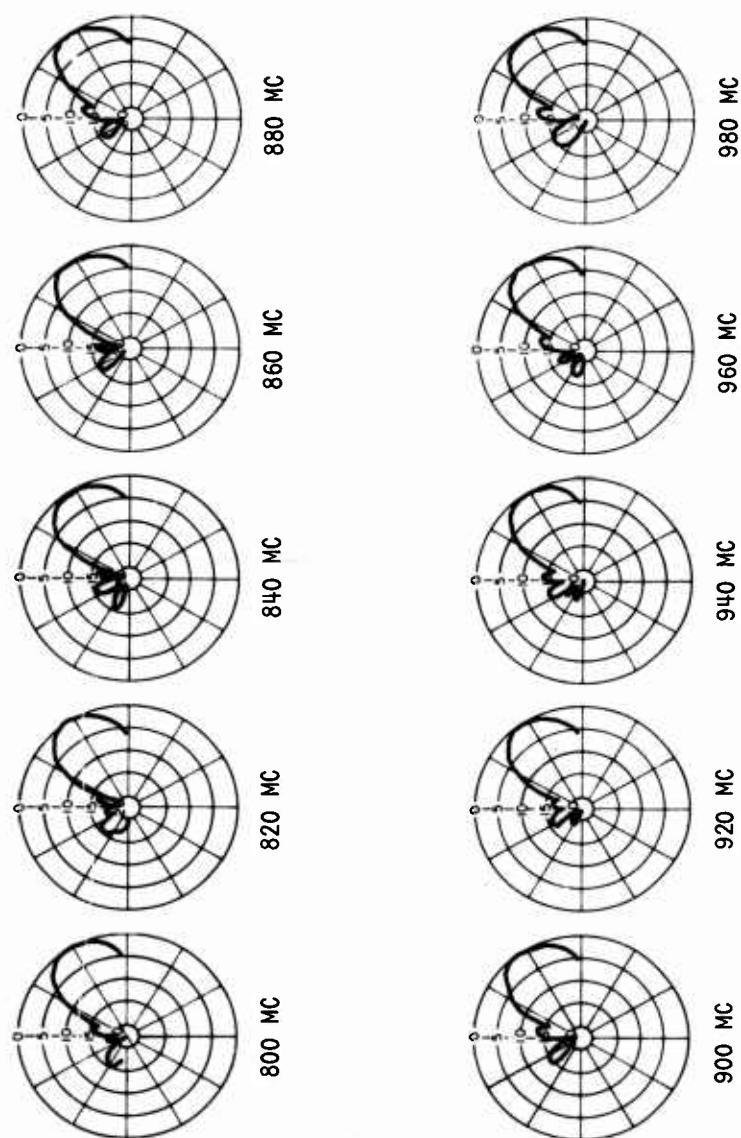


Figure 16. E-plane Radiation Power Patterns of a Log Periodic Monopole Array with Parasitic Elements ( $\tau = 0.886$ ,  $s/l = 0.0568$ ).

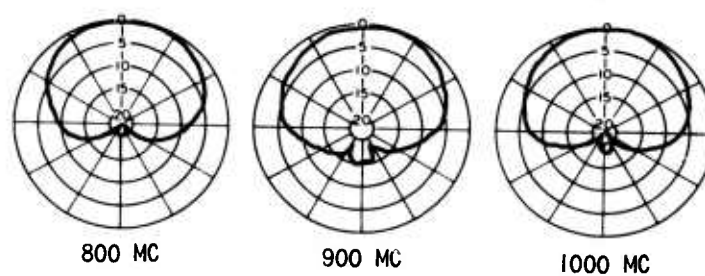


Figure 17. H-plane Radiation Power Patterns of a Log Periodic Monopole Array with Parasitic Elements (20-degree conical cut) ( $\tau = 0.889$ ,  $s/\ell = 0.0568$ ).

### 6.1 -- Continued.

elements. The results of this experiment showed that the mutual coupling between the parasitic element and driven element was too low, thus indicating that there is a lower limit to the value of  $\tau$  that can be used with this class of antennas.

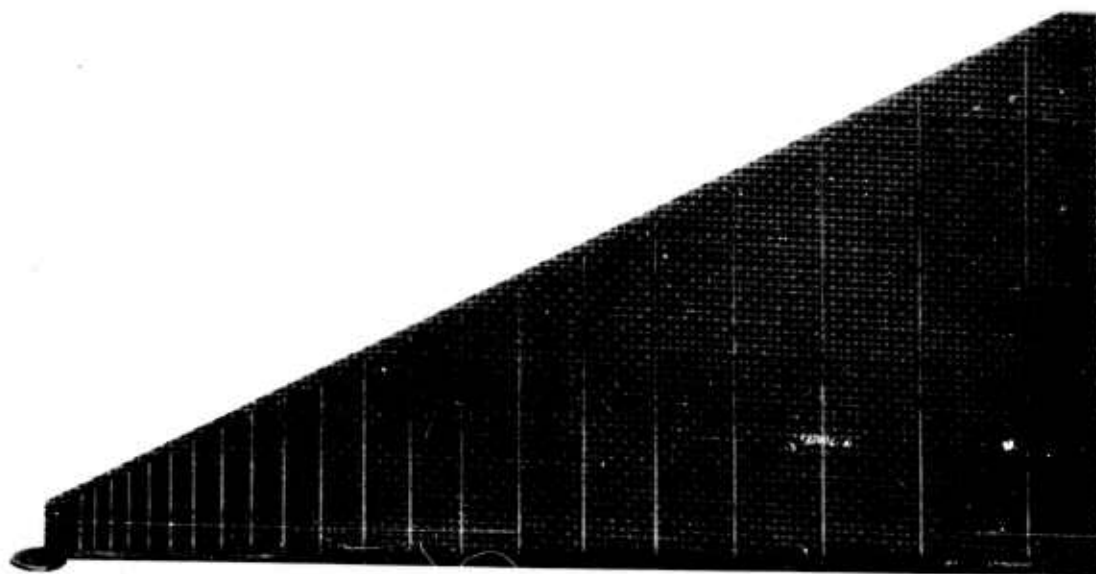
An additional experiment of interest was performed where the parasitic elements of the first antenna discussed in this section were disconnected from the ground plane. This configuration of the antenna failed to work in a frequency-independent manner.

### 6.2 Microwave Model.

A microwave version of the log periodic monopole antenna with parasitic elements was designed to operate from S-band through X-band frequencies. A design ratio of 0.889 and element-spacing-to-length ratio of 0.0557 was used. The antenna itself was etched on a double clad printed circuit board with the driven elements and the feeder line etched on one side, as shown in Figure 18A. The connection at the feed can be seen in this illustration. The parasitic elements are etched on the opposite side and are shown soldered to the ground plane in Figure 18B. The longest element of the antenna is 1.556 inches in length and the shortest element is 0.191 inches in length. A modified connector was used for the feed which stepped the type-N coaxial size to a subminiature coaxial size while maintaining a 50-ohm characteristic impedance. This was done to prevent radiation from the feed itself.

The characteristics of this antenna were measured and found to be pseudo-frequency independent. An impedance circle of about 50 ohms with a VSWR of 3:1 was measured from 1.5 Gc to 12.6 Gc. Radiation-pattern measurements were also obtained over this frequency range. Some of the E-plane and H-plane (20-degree conical cut) radiation-power patterns are shown in Figures 19 and 20. These radiation patterns have essentially constant beamwidths with a constant vertical take-off angle over the entire frequency range and with a front-to-back ratio of about 15 db. The serrations in the radiation patterns are primarily caused by the limited ground plane on which the antenna was mounted for the measurements.

This log periodic antenna is well suited for microwave applications in that it provides good electrical performance in this frequency range and is inexpensive to construct. Good performance is possible primarily because of the simplicity of feeding the antenna. No special coaxial transformers are required, and there is no need for coaxial lines or other components in the vicinity of the element (such components would be a large percentage of

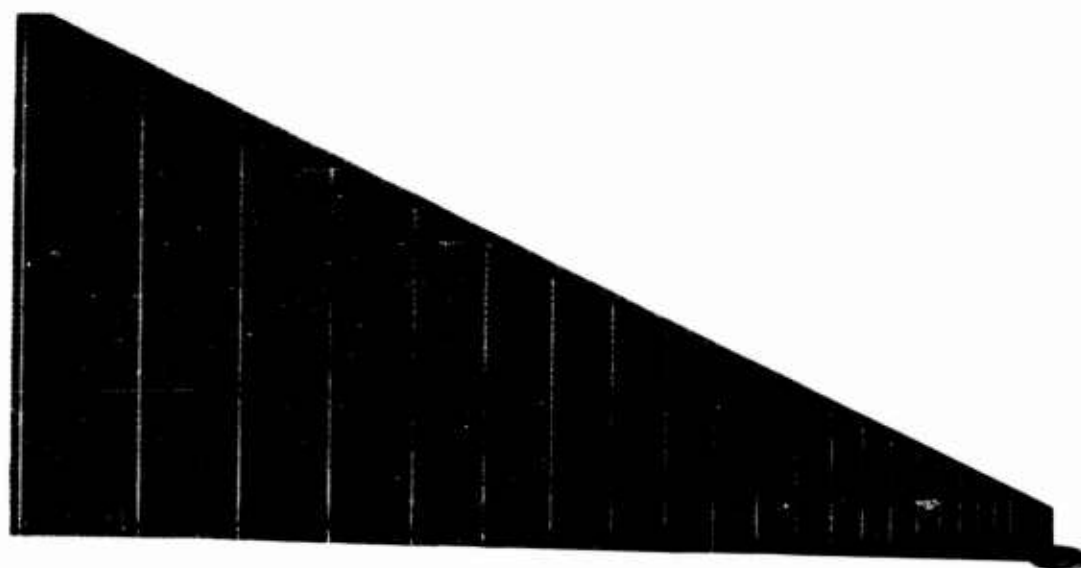


61120812

Figure 18. Microwave Model of a Log Periodic Monopole Array with Parasitic Elements ( $\tau \approx 0.898$ ,  $s/\ell \approx 0.0557$ ).



EDL-M623



61120813

Figure 18. -- Continued.

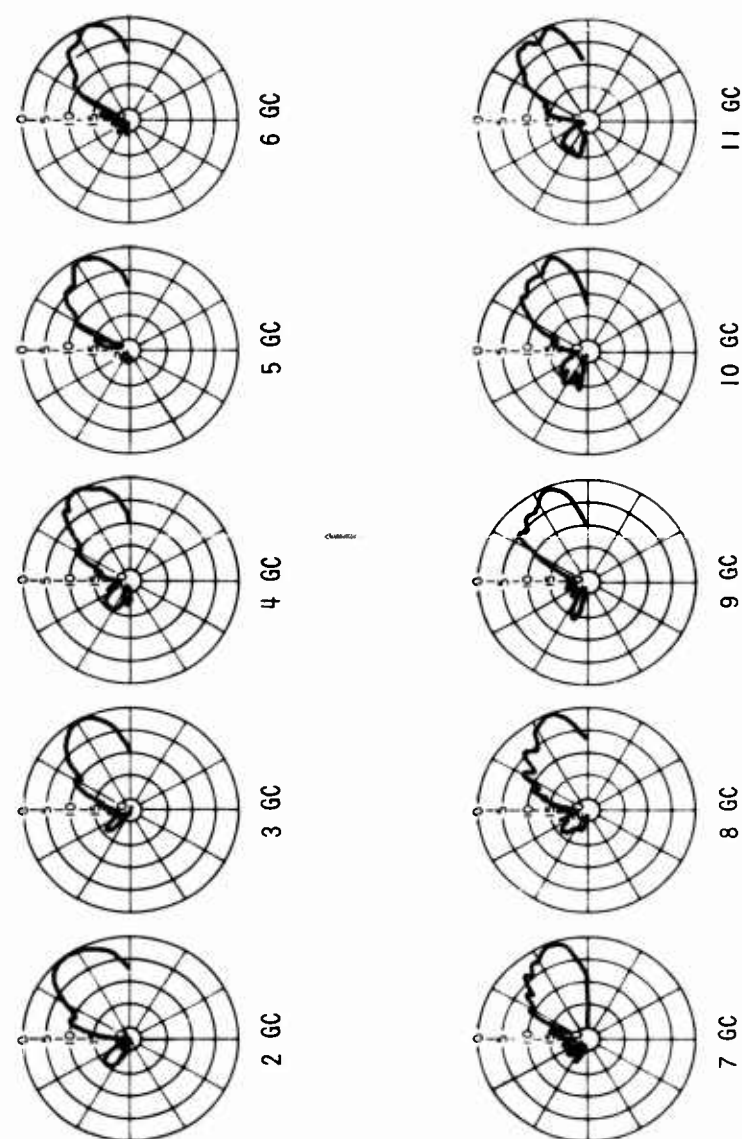


Figure 19. E-plane Radiation Power Patterns of a Log Periodic Monopole Array with Parasitic Elements ( $\tau \approx 0.898$ ,  $s/\ell = 0.0557$ ).

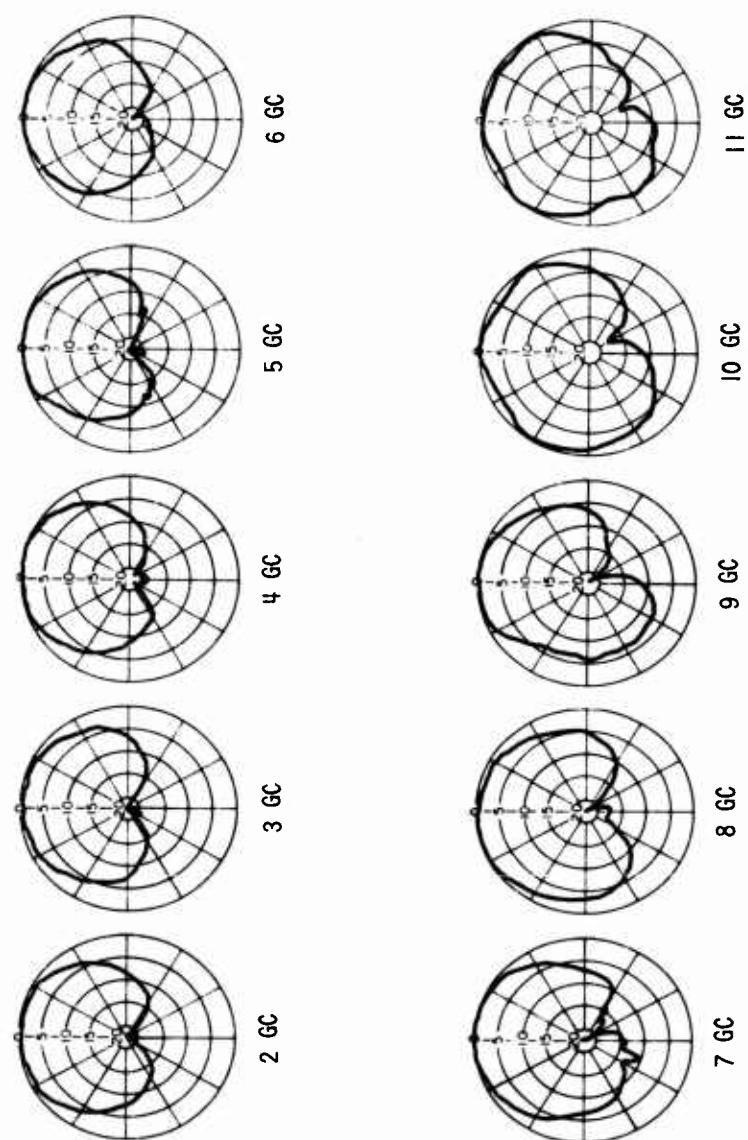


Figure 20. H-plane Radiation Power Patterns of a Log Periodic Monopole Array with Parasitic Elements ( $\tau \approx 0.898$ ,  $s/\ell \approx 0.0557$ ).

6.2                      Continued.

the size of the smallest element). The independence from any form of capacitive coupling eliminates the need for critical spacings.

## 7. CONCLUSION.

The log periodic dipole and monopole arrays with parasitic elements have been introduced and their characteristics presented. It was shown that the method of feeding these antennas is relatively simple, thus making the antennas suitable for frequency ranges that are difficult to cover with other log periodic antennas. It was also shown that an antenna having more than one parasitic element between each driven dipole element will work as a pseudo frequency-independent antenna. In this respect, there exist numerous configurations and possibilities with the dipole or monopole arrays having multiparasitic elements. A limitation on the log periodic dipole or monopole array with parasitic elements is that larger values of  $\tau$  must be used in comparison with other log periodic antennas. As a result, this antenna will always have a high density of elements.

It appears probable that a log periodic Yagi antenna design might evolve from the log periodic dipole array with parasitic elements. In the multiparasitic element design discussed above, the apparent source of radiation appeared to be confined to the cells of the antenna rather than to the individual elements themselves. This effect occurs when the cells, not the elements, are log periodic in nature. The cells of this antenna can be made to conform to a Yagi antenna design. It is conceivable that a log periodic antenna of this design can be made to work satisfactorily, and further experiments to investigate this are necessary.

8. REFERENCES

1. D. E. Isbell, "Log Periodic Dipole Arrays", IRE Trans. on Antennas and Propagation, Volume AP-8, No. 3, May, 1960; pp 260-270. (UNCLASSIFIED publication)
2. R. Mittra, "Theoretical Study of a Class of Logarithmically Periodic Circuits", Technical Report No. 59, Antenna Laboratory, University of Illinois; July 1962. (UNCLASSIFIED publication)
3. P. E. Mayes, G. A. Deschamps, and W. T. Patton, "Backward-Wave Radiation from Periodic Structures", Technical Report No. 60, Antenna Laboratory, University of Illinois; December 1962. (UNCLASSIFIED publication)
4. A. A. Oliner, "Leaky Waves in Electromagnetic Phenomena", Research Report No. PIBMRI-1064-62, Polytechnic Institute of Brooklyn; August 1962. (UNCLASSIFIED publication)
5. R. Mittra and K. E. Jones, "Theoretical Brillouin ( $k$ - $\beta$ ) Diagram for Monopole and Dipole Arrays and Their Application to Log Periodic Antennas", 1963 IEEE International Convention Record, Part 1; 25-28 March 1963, pp 118-128. (UNCLASSIFIED publication)
6. E. Hudock and P. E. Mayes, "Propagation Along Periodic Monopole Arrays", 1963 PTGAP International Symposium; 9-11 July 1963; pp 127-132. (UNCLASSIFIED publication)
7. C. T. Elfving, "Design Criteria for Log Periodic Antennas", 1961 WESCON, Paper 1/2; 22-25 August 1961. (UNCLASSIFIED publication)
8. H. Jasik, "Antenna Engineering Handbook", McGraw Hill Book Company, Inc.; 1961; pp 5-6 to 5-11. (UNCLASSIFIED publication)
9. P. Toullos, "RFD Antenna Techniques Survey" (U), Final Report, Volume 1, Armour Research Foundation of Illinois Institute of Technology, Chicago, Illinois; 19 December 1961. (SECRET publication), pp 65-72.
10. D. G. Berry and F. R. Ore, "Log Periodic Monopole Array", 1961 IRE International Convention Record, Part I; 20-23 March 1961; pp 76-85. (UNCLASSIFIED publication)

(iv + 36)

AD	Accession No.	UNCLASSIFIED	Copy No.
AD	Electronic Defense Labs., Mountain View, Calif. LOG PERIODIC DIPOLE ARRAY WITH PARASITIC ELEMENTS -- Normand Barbano, Technical Memorandum EDL-M623, 30 January 1964 (Contract DA 36-039 AMC-00088(E)) UNCLASSIFIED Report.	1. *Log 2. *Periodic 3. *Dipole 4. *Array 5. *Parasitic 6. *Element 7. Spacing 8. *Monopole 9. *Antenna 10. Two 11. Wire 12. Feeder 13. Phase 14. Brillouin 15. Radiation 16. Pattern 17. Forward 18. Backward 19. Wave 20. Backfire 21. Fire 22. Impedance	UNCLASSIFIED 1. *Log 2. *Periodic 3. *Dipole 4. *Array 5. *Parasitic 6. *Element 7. Spacing 8. *Monopole 9. *Antenna 10. Two 11. Wire 12. Feeder 13. Phase 14. Brillouin 15. Radiation 16. Pattern 17. Forward 18. Backward 19. Wave 20. Backfire 21. Fire 22. Impedance
AD	Electronic Defense Labs., Mountain View, Calif. LOG PERIODIC DIPOLE ARRAY WITH PARASITIC ELEMENTS -- Normand Barbano, Technical Memorandum EDL-M623, 30 January 1964 (Contract DA 36-039 AMC-00088(E)) UNCLASSIFIED Report.	The design and measured characteristics of dipole and monopole versions of a log periodic array with parasitic elements are discussed. In a dipole array with parasitic elements, these elements are used in place of every alternate dipole, thereby eliminating the need of a twisted feed arrangement for the elements to obtain log periodic performance of the antenna. This design with parasitic elements lends itself to a monopole version of the antenna which has a simplified feeding configuration. The result is a log periodic antenna design that can be used from high frequencies through microwave frequencies.	UNCLASSIFIED 1. *Log 2. *Periodic 3. *Dipole 4. *Array 5. *Parasitic 6. *Element 7. Spacing 8. *Monopole 9. *Antenna 10. Two 11. Wire 12. Feeder 13. Phase 14. Brillouin 15. Radiation 16. Pattern 17. Forward 18. Backward 19. Wave 20. Backfire 21. Fire 22. Impedance
AD	Electronic Defense Labs., Mountain View, Calif. LOG PERIODIC DIPOLE ARRAY WITH PARASITIC ELEMENTS -- Normand Barbano, Technical Memorandum EDL-M623, 30 January 1964 (Contract DA 36-039 AMC-00088(E)) UNCLASSIFIED Report.	The design and measured characteristics of dipole and monopole versions of a log periodic array with parasitic elements are discussed. In a dipole array with parasitic elements, these elements are used in place of every alternate dipole, thereby eliminating the need of a twisted feed arrangement for the elements to obtain log periodic performance of the antenna. This design with parasitic elements lends itself to a monopole version of the antenna which has a simplified feeding configuration. The result is a log periodic antenna design that can be used from high frequencies through microwave frequencies.	UNCLASSIFIED 1. *Log 2. *Periodic 3. *Dipole 4. *Array 5. *Parasitic 6. *Element 7. Spacing 8. *Monopole 9. *Antenna 10. Two 11. Wire 12. Feeder 13. Phase 14. Brillouin 15. Radiation 16. Pattern 17. Forward 18. Backward 19. Wave 20. Backfire 21. Fire 22. Impedance

UNCLASSIFIED Copy No.

- 23. Ultra-High-Frequency
- 24. Microwave
- 25. Transmission
- 26. Line

I. Barbano, Normand  
II. Contract DA 36-039  
AMC-00088 (E)

8.1: 8.6

UNCLASSIFIED Copy No.

- 23. Ultra-High-Frequency
- 24. Microwave
- 25. Transmission
- 26. Line

I. Barbano, Normand  
II. Contract DA 36-039  
AMC-00088 (E)

8.1: 8.6

UNCLASSIFIED Copy No.

- 23. Ultra-High-Frequency
- 24. Microwave
- 25. Transmission
- 26. Line

I. Barbano, Normand  
II. Contract DA 36-039  
AMC-00088 (E)

8.1: 8.6

UNCLASSIFIED Copy No.

- 23. Ultra-High-Frequency
- 24. Microwave
- 25. Transmission
- 26. Line

I. Barbano, Normand  
II. Contract DA 36-039  
AMC-00088 (E)

8.1: 8.6